APPLICATIONS OF
MODELLING AND SIMULATION
http://arqiipubl.com/ams eISSN 2600-8084 VOL 3, NO. 1, 2019, 11-17

A Flexible Rope Crane Experiment System

R. Yang, C. Jiang, Y. Miao, J. Ma, X. Zhang, T. Yang and N. Sun

College of Artificial Intelligence, Nankai University, Tianjin 300350, China.

*Corresponding author: yangt@mail.nankai.edu.cn

Submitted 23 November 2018, Revised 5 January 2019, Accepted 7 January 2019.

Abstract: In many cases, overhead cranes will exhibit flexible rope dynamics and precise control of such cranes is difficult to obtain, due to unexpected curving of the flexible rope. To study the dynamics of flexible rope cranes and to test the effectiveness of various controllers, a flexible rope crane experiment system is established according to the working principles of practical cranes. The experiment system is composed of a mechanical body, driving devices, measuring devices, and a control system. Additionally, in order to quantitatively evaluate the control performance, this paper proposes a method combining vision inspection and machine learning to obtain the rope curve model and measure the pendulum angle at the end of the rope. The control system is established on the MATLAB/Simulink platform and various automatic control strategies can be easily applied to it.

Keywords: Automatic control; Experiment system; Flexible rope crane; Machine learning; Vision inspection.

1. INTRODUCTION

In transportation and manufacturing fields, overhead cranes are a kind of important transportation tools, which can move cargos to target positions quickly and accurately [1-3]. They are widely applied in industrial situations, such as production workshops, installation sites, etc. However, overhead cranes are typical nonlinear underactuated systems, whose degrees-of-freedom (DOFs) are more than the number of control inputs [4]. Due to the underactuated feature, the uneven and fast trolley motion will cause large payload sway, i.e., the swing angle at the top of the rope (hereafter called the top angle). Therefore, it is difficult to achieve trolley positioning and payload sway elimination simultaneously [5]. To overcome the above problems, a lots of researches contribute to presenting automatic control technology [6-9].

In the literature, most existing researches consider the rope as rigid. However, flexible rope cranes are also widely used in practice and exhibit many advantages over their rigid counterparts [10]. Since ropes are flexible, they will generate non-negligible curving. Especially when the rope length is up to tens of meters and some external factors like strong wind and ocean current disturbances happen to cranes [11-12], the rope curving will become non-negligible, so that it will generate a pendulum angle at the end of the rope (hereafter called the end angle) [13]. Hence, the rope cannot be viewed as rigid; otherwise it will lead to the deviation between the ideal result and the practical application. The above issues are very likely to cause safety accidents when operating flexible rope cranes.

Currently, flexible rope cranes have generated great interest in the field of control. Most researches on flexible rope cranes mainly focus on two kinds of control problems [14-15]. On one hand, it is necessary to realise fast and accurate positioning of trolleys; on the other hand, it is necessary to quickly and effectively suppress both payload swing and rope curving. The difficulty of flexible rope crane control is that the rope curving will generate the end angle, which is different from rigid rope crane control. In order to achieve ideal swing elimination of the entire rope, it is pivotal to obtain the end angle as a quantitative evaluation index. However, there are few researches focusing on the measurement of the end angle. Therefore, this paper designs an experiment system, which can imitate the operation of practical flexible rope cranes. Additionally, a method combining vision inspection and machine learning is proposed to obtain the rope curve model and measure the end angle, which is used to quantitatively evaluate the control performance.

2. SYSTEM DESIGN AND IMPLEMENTATION

According to the working principle and composition of practical flexible rope cranes, the experiment system in this paper is composed of a mechanical body, driving devices, measuring devices, and a control system (see Figure 1).

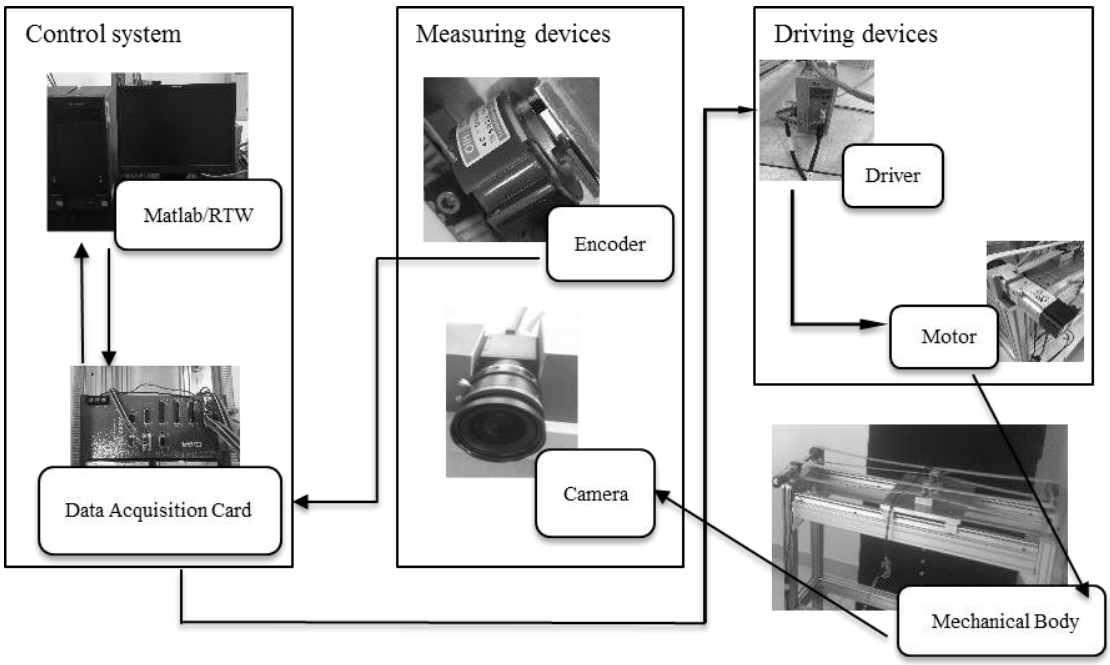

Figure 1. Experiment system of a flexible rope crane

The mechanical body refers to the main mechanical part of the flexible rope crane. The driving devices, i.e., a servo motor, can provide a corresponding force to the mechanical body according to the control signals. Control signals can be calculated based on the crane dynamic model and real-time state feedback. The system states are obtained by the measuring devices, which convert the system states, such as the trolley position and the top angle, into corresponding electrical signals through the sensing devices. Then these electrical signals are sent to the control system. Additionally, the system can use a method combining vision inspection and machine learning to obtain the rope curve model offline. Thus, the end angle can be obtained, which is used to quantitatively evaluate the control performance.

2.1 Mechanical Body and Driving Devices

The mechanical body is the main part of the whole experiment system. It is designed according to the structure of practical flexible rope crane systems, including a support frame, a trolley, a flexible rope, and a payload (see Figure 2).

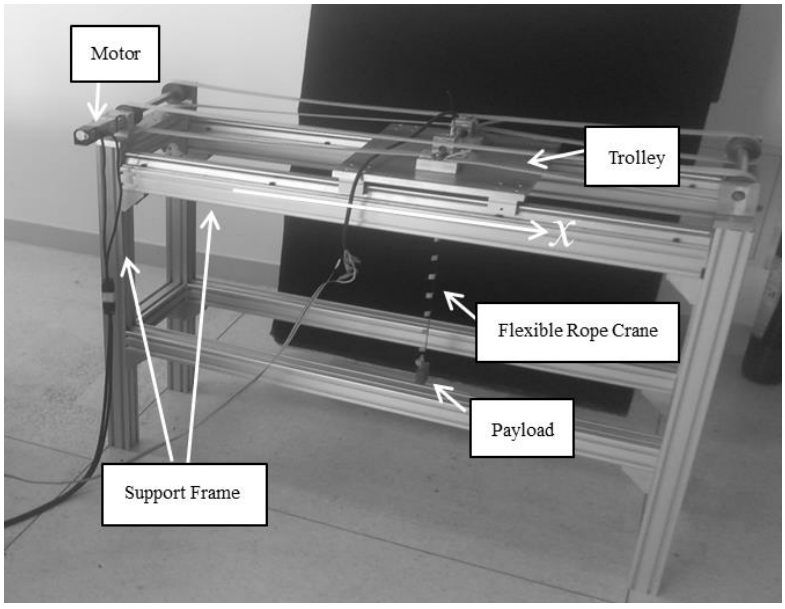

Figure 2. Mechanism of the experiment system

The driving devices mainly include a servo motor (see Figure 2), which can drive the trolley in the horizontal direction by the synchronous wheel and the synchronous belt. In hardware experiments of flexible rope cranes, an AC servo motor is used, which has the advantages of large output power and convenient maintenance, to control the experiment system.

2.2 Measuring Devices

The measuring devices are responsible for measuring three state variables of the flexible rope crane, i.e., the trolley position on x axis, the top angle, and the end angle.

2.2.1 Position Measurement

The trolley position x can be calculated by encoder included in the AC servo motor [16]:

$$\Delta x = \frac{N_1 \times C}{F \times P \times R} \tag{1}$$

where N_1 is the reading of the AC servo motor's encoder, C is the circumference of the synchronous wheel, F is the double frequency of acquisition card, P is the resolution of encoder (pulse per round), and R is the reduction ratio of reducer.

2.2.2 Top Angle Measurement

The top angle of the slope can be measured by a rotary encoder, which is denoted by θ_1.In Figure 3, the semicircular light swing frame can rotate around the rotation axis, and the rotation axis lies on a plane parallel to the horizontal plane. One end of the rotary shaft is equipped with a rotary encoder for measuring the rotation angle of the swing frame. There is a smooth slit in the middle of the semicircular swing frame, and the rope passes through the slit and is fixed to the locating hole, so that when the rope is swinging, the swing frame will be driven to rotate. Then the top angle θ_1 can be obtained. The formula for calculation is as follows [16]:

$$\Delta\theta_1 = \frac{N_2 \times 2\pi}{F \times P} \tag{2}$$

where N_2 is the reading of rotary encoder.

2.2.3 End Angle Measurement

A flexible steel sheet with 0.6 meters long and 0.015 meters wide is selected as the rope in this paper, so that the curving of the steel sheet itself will be relatively notable during the movement of the trolley. The crooked steel sheet will generate a pendulum angle at the end of the rope (the end angle), which is denoted by θ_2. The schematic diagram of the end angle is shown in Figure 4: take any point of the rope near the payload and make the tangent of the point. The angle between the tangent and plumb line is the end angle θ_2.

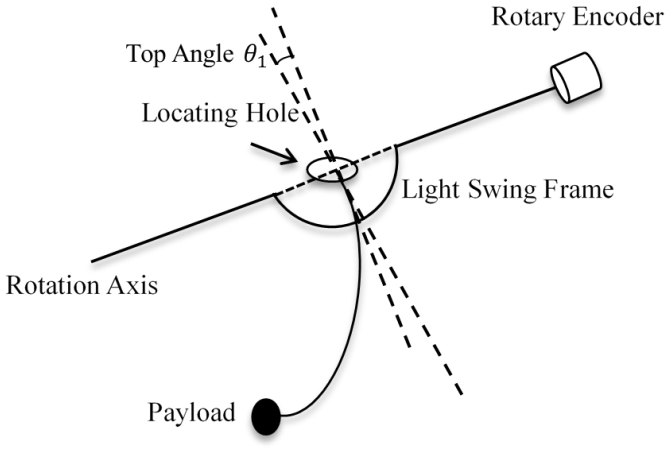

Figure 3. Top angle measurement device

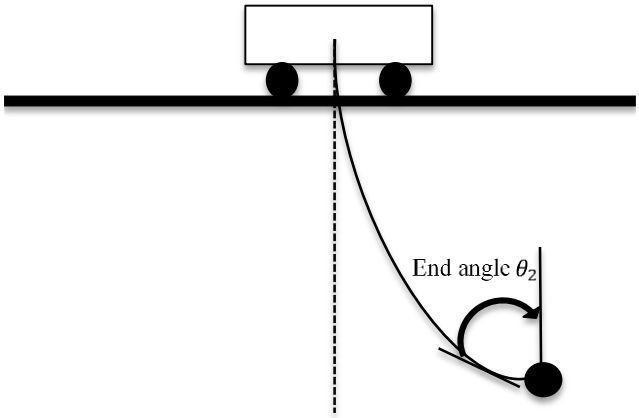

Figure 4. The schematic diagram of the end angle

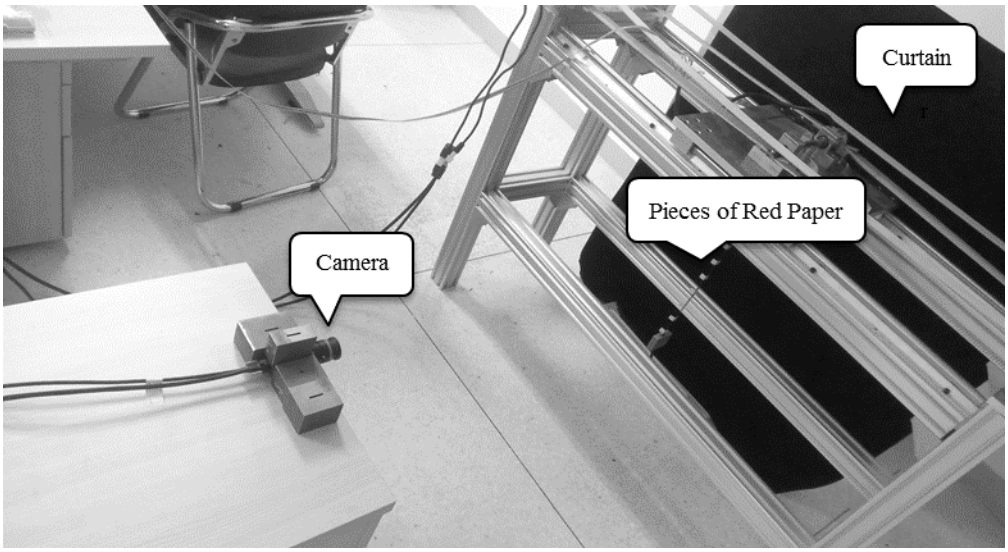

Figure 5. Vision inspection device

Then, this paper obtains a nonlinear relationship between the top angle and the end angle offline by a method combining vision inspection and machine learning. In the process of trolley movement, the value of the top angle measured by the rotary encoder is added into this relationship, and the value of the end angle can be obtained as quantitative evaluation of the control performance. Considering the fixed linear relationship between the top angle and the rotary encoder reading (see Equation (2)), this paper directly establishes the relationship between the rotary encoder reading and the end angle.

The steps for vision inspection are as follows:

(1) Pieces of red paper are attached every 0.05 meters on one side of the steel sheet as feature points for vision inspection.

(2) Place a black curtain at the back of the experiment system as the background and an industrial camera in the front.

A Hikvision camera with a resolution of 1280×1024 and a maximum acquisition frame rate of 36.04 is used in this paper. The vision inspection device is shown in Figure 5.

(3) Record multiple sets of swing video and the corresponding rotary encoder readings.

(4) Use both dynamic inspection and static inspection methods to obtain the pixel coordinates (x, y) of the feature points in each frame.

Static inspection method refers to splitting the videos into independent video frames, processing the frames into binary images using color thresholding in RGB space, and using function *Regionprops()* in MATLAB to detect each piece of red paper. By using *Camshift* method in OpenCV [17], dynamic inspection method can convert RGB space to HSV space, combined with probability distribution and object tracking, to achieve successful inspection of the feature points.

(5) According to the time domain alignment principle, the rotary encoder readings are in one-to-one correspondence with the pixel coordinates to construct the original dataset.

In order to correspond the frame inspection results to the rotary encoder readings, a time domain interpolation method is

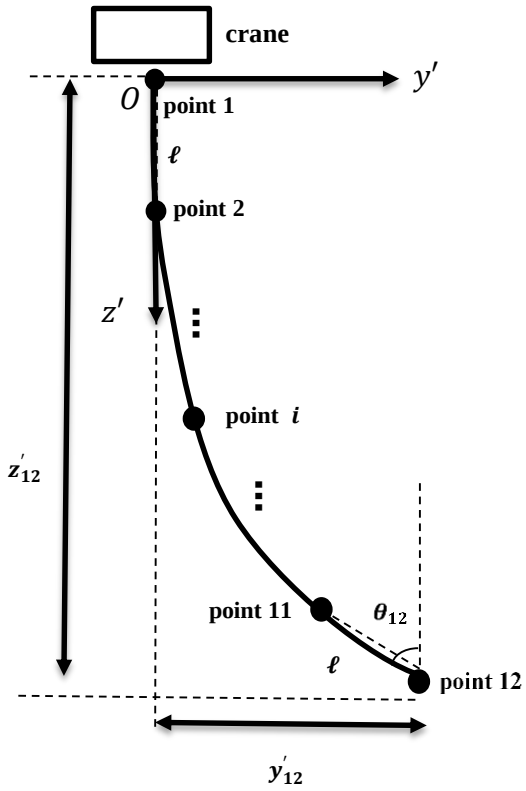

Figure 6. Coordinate conversion relationship

adopted, since the sampling frequency of the rotary encoder is much higher than the camera frame rate. The starting frame is aligned with the corresponding rotary encoder reading by the dataset's line number, and so is the ending frame. Then all the frames are equally spaced according to the time axis, and the line number corresponding to the rotary encoder readings for each frame is obtained. After obtaining the pixel coordinates (x, y), they are converted into the world coordinates (z', y', θ), for subsequent machine learning. The coordinate conversion relationship [18] is shown in Figure 6.

In Figure 6, the pixel coordinates of the feature point i are (x_i, y_i), The distance between the feature points $i-1$ and i is l, which is 0.05 meters in this paper. Since the camera shooting does not change the relative position between the feature points, the relationship between pixel coordinates (x_i, y_i) and the world coordinates (z'_i, y'_i, θ_i) can be established as follows:

$$\begin{cases} \theta_i = arctan\frac{y_i - y_{i-1}}{x_i - x_{i-1}} \\ z'_i = z'_{i-1} + \ell\cos\theta_i \\ y'_i = y'_{i-1} + \ell\sin\theta_i \end{cases} \tag{3}$$

where z'_i is the vertical distance between the feature point i and the trolley, y'_i is the horizontal distance between the feature point i and the suspension point of the rope, and θ_i is the angle between the tangent and plumb line at the feature point i, which can be replaced by the angle between the line connecting the feature points i and $i-1$ and the plumb line.

Specially in this paper, according to the schematic diagram shown in Figure 4, the swing angle θ_{12} of the feature point 12 is defined as the end angle θ_2. Without loss of generality, the initial values of (z'_1, y'_1, θ_1) are selected as follows:

$$\begin{cases} \theta_1 = 0 \\ y'_1 = 0 \\ z'_1 = 0 \end{cases} \tag{4}$$

Then, machine learning will be introduced to train the relationship between the rotary encoder reading and the end angle. The concrete procedures are as follows:

(1) Get the needed training data for machine learning method by the rotary encoder and vision inspection.
The input data is the rotary encoder reading N_2, and the output data is the world coordinates of each feature point (z'_i, y'_i, θ_i).

(2) Train a specific nonlinear function offline by the regression tree model [19-20] in machine learning.
The regression tree model is an algorithm of machine learning to fit a nonlinear function. It uses other fitting algorithms such as linear fitting algorithm to fit a specific function, based on relatively simple communities obtained by dividing

the complex training data. Considering that θ_1 is calculated from the rotary encoder, this paper directly establishes the nonlinear function between the rotary encoder reading N_2 and the world coordinates (z_i', y_i', θ_i) of each feature point. The rotary encoder reading N_2 and the corresponding world coordinates (z_i', y_i', θ_i) are grouped into a set of sample data and trained by a regression tree model. Then the rope curve model, which is actually a nonlinear function, is obtained offline.

(3) Code the model into a program in C++ language.

After the curve model is obtained offline, the function is coded into a program. By inputting the rotary encoder reading N_2, this program can get the corresponding end angle θ_2 in real time, thus making closed-loop control based on it feasible.

It is worthwhile to point out that when the length and material of the rope are changed, the existing curve model will no longer apply. At this time, we can re-perform the procedures of vision inspection and machine learning to get a new effective curve model.

2.3 Control System

In order to achieve effective control, it is necessary to measure the state variables by sensors in real time and accurately convey the control inputs to servo motors. Therefore, a high real-time environment is required to complete the control objectives.

Considering that the experiment system in this paper needs high real-time control performance to facilitate the realization and debugging of the control algorithm, a real-time environment based on MATLAB RTW is selected, which has the following advantages [21]: 1) It can automatically generate high-frequency code for different object platforms; 2) It can be seamlessly connected to MATLAB/Simulink, so it can easily realise various control algorithms; 3) It can facilitate the design processes and application.

MATLAB RTW supports multiple experimental platforms; hence, RealTime Windows Target (RTWT), a real-time control platform under Windows, is selected in this paper. It only needs one PC and can realise real-time control of the system with a control period of 5 ms. In addition, the control system includes a motion control board, which obtains the trolley position and the top angle and sends them to the PC. The control signals calculated by the PC are later sent to the driving devices.

3. EXPERIMENTAL RESULTS

In order to test the method combining vision inspection and machine learning proposed in this paper, a series of data groups of top angle are randomly collected from the experiment system. By inputting them into the program (the curve model), the corresponding data of end angle is output in real time. Actually, the average operation time is within 2 ms, which can definitely realise real-time control of the MATLAB system with a control period of 5 ms.

Due to space limitation, only one data group of both the top angle and the end angle is presented. The experimental results are shown in Figure 7. It can be seen from the experimental results that by utilising the proposed method, the end angle can be obtained in real time for quantitative evaluation and automatic control.

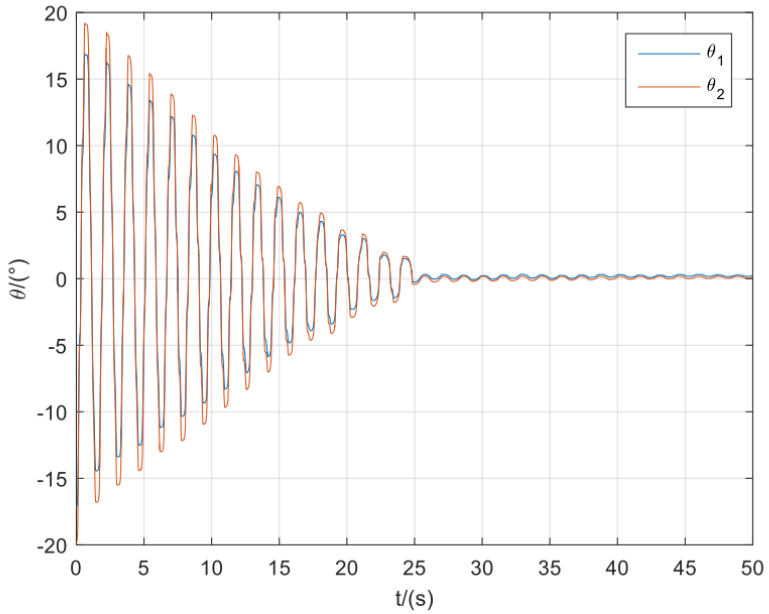

Figure 7. Experimental results of top angle θ_1 and end angle θ_2

4. CONCLUSION

In order to study the dynamic model of flexible rope cranes and verify various controllers, a flexible rope crane experiment system is established in this paper. The experiment system is composed of a mechanical body, driving devices, measuring devices, and a control system. It can imitate the operation of practical flexible rope cranes and based on the MATLAB/Simulink platform, it is convenient to carry out validations for various control strategies. Different from rigid rope crane control, effective control of flexible rope cranes is more difficult to achieve, due to the rope flexibility. Apart from the top angle caused by the cranes' motions, large curving of the flexible rope will generate the end angle. Moreover, the measurement of the end angle is a vital quantitative evaluation of cranes' control performance. However, it is hard to obtain the end angle, because it cannot be directly measured by an encoder. Therefore, this paper proposes a method combining vision inspection and machine learning to obtain the rope curve model and measure the end angle. Our future work will be dedicated to applying various control strategies to the experiment system and quantitatively evaluating the control performance by the end angle. Considering the proposed method is not limited to flexible rope crane experiment systems, the method to implement measurements will be extended in other experiment systems.

REFERENCES

[1] H. Ouyang, G. Zhang, L. Mei and X. Deng, Vibration reduction for human-operated overhead cranes using S-shaped motion trajectory, *Chinese Control Conference*, Chengdu, China, 2016, pp. 6144–6147.

[2] M. Zhang, X. Ma, X. Rong, R. Song, X. Tian and Y. Li, A partially saturated adaptive learning controller for overhead cranes with payload hoisting/lowering and unknown parameters, *Nonlinear Dynamics*, 89(3), 1779–1791, 2017.

[3] N. Sun and Y. Fang, New energy analytical results for the regulation of underactuated overhead cranes: An end-effector motion-based approach, *IEEE Transactions on Industrial Electronics*, 59(12), 4723–4734, 2012.

[4] N. Sun, Y. Fang, H. Chen and B. Lu, Amplitude-saturated nonlinear output feedback antiswing control for underactuated cranes with double-pendulum cargo dynamics, *IEEE Transactions on Industrial Electronics*, 64(3), 2135–2146, 2017.

[5] N. Sun, Y. Fang, Y. Zhang and B. Ma, A novel kinematic coupling-based trajectory planning method for overhead cranes, *IEEE/ASME Transactions on Mechatronics*, 17(1), 166–173, 2012.

[6] B. Ma, *Research on automatic control of an under-actuated nonlinear bridge crane system*, Ph.D. dissertation, Control Theory and Engineering, Nankai University, Tianjin, 2009.

[7] L. Ramli, Z. Mohamed, A. M. Abdullahi, H. I. Jaafar and I. M. Lazim, Control strategies for crane systems: A comprehensive review, *Mechanical Systems and Signal Processing*, 95, 1–23, 2017.

[8] M. J. Maghsoudi, Z. Mohamed, S. Sudin, S. Buyamin, H. I. Jaafar and S. M. Ahmad, An improved input shaping design for an efficient sway control of a nonlinear 3D overhead crane with friction, *Mechanical Systems and Signal Processing*, 92, 364–378, 2017.

[9] N. Sun, Y. Fang and X. Zhang, Energy coupling output feedback control of 4-DOF underactuated cranes with saturated inputs, *Automatica*, 49(5), 1318–1325, 2013.

[10] Z. Mohamed, J. Martins, M. Tokhi, J. Da Costa and M. Botto, Vibration control of a very flexible manipulator system, *Control Engineering Practice*, 13(3), 267–277, 2005.

[11] L. Tuan, H. Cuong, P. Trieu, L. Nho, V. Thuan and L. Anh, Adaptive neural network sliding mode control of shipboard container cranes considering actuator backlash, *Mechanical Systems and Signal Processing*, 112, 233–250, 2018.

[12] W. He, S. Ge, B. How, Y. Choo and K. Hong, Robust adaptive boundary control of a flexible marine riser with vessel dynamics, *Automatica*, 47(4), 722–732, 2011.

[13] S. Park, B. K. Kim and Y. Youm, Single-mode vibration suppression for a beam–mass–cart system using input preshaping with a robust internal-loop compensator, *Journal of Sound and Vibration*, 241 (4), 693–716, 2001.

[14] W. He, S. Zhang and S. Ge, Adaptive control of a flexible crane system with the boundary output constraint, *IEEE Transactions on Industrial Electronics*, 61(8), 4126–4133, 2014.

[15] W. He and S. Ge, Cooperative control of a nonuniform gantry crane with constrained tension, *Automatica*, 66, 146–154, 2016.

[16] B. Ma, Y. Fang, P. Wang and Y. Yuan, Experiment system for automatic control of a 3D bridge crane, *Control Engineering of China*, 18(2), 239–243, 2011.

[17] L. Ye and Y. Wang, Real-time tracking of the shoot point from light pen based on camshift, *International Conference on Intelligent Networks and Intelligent Systems*, Wuhan, China, 2008, pp. 560–564.

[18] P. S. Gandhi, P. Borja and R. Ortega, Energy shaping control of an inverted flexible pendulum fixed to a cart, *Control Engineering Practice*, 56, 27–36, 2016.

[19] J. Rothwell, M. Futter and N. Dise, A classification and regression tree model of controls on dissolved inorganic nitrogen leaching from european forests, *Environmental Pollution*, 156(2), 544–552, 2008.

[20] A. Dobra and J. Gehrke, SECRET: A scalable linear regression tree algorithm, *Eighth ACM SIGKDD International Conference on Knowledge Discovery and Data Mining*, Alberta, Canada, 2002, pp. 481–487.

[21] Z. Song, J. Wang, C Liu and X. Song, Design of a hardware-in the loop experiment simulation system for process control based on RTW, *2009 First International Workshop on Education Technology and Computer Science*, Wuhan, China, 2009, pp. 1123–1126.